

Supporting Information

An Extraordinary Boron-Mediated 16R-Channel-Containing Trivalent Vanadium Phosphite with Unique Solid State Redox Property

Table S1. Crystal data for compound **1**

Table S2. Selected Bond Length (Å) for **1**

Table S3. ICP-AES data

Figure S1. TG curves of compound **1**

Figure S2. Variable-temperature powder X-ray diffraction patterns of compound **1**.

Figure S3. (a) Reflectance UV-vis spectra, and (b) photoluminescence spectra of compound **1**.

Figure S4. Plots of (a) χ_M versus T , and (b) χ_M^{-1} versus T curves of **1**.

Figure S5. Plots of (a) χ_M^{-1} versus T , and (b) $\chi_M T$ versus T curves of **1** and **1T**.

Figure S6. Simulated (bottom) and experimental (top) X-ray powder patterns for **1**, and the magnification part of the simulated pattern at 19.3° is shown in the inset.

Figure S7. Comparable simulated (bottom) and experimental (top) powder patterns of **1** and the isostructure of **1**, respectively.

Figure S8. FTIR spectrum for **1**.

Table S1. Crystal data for compound **1**

Empirical formula	$V_9P_{16.57}B_{0.43}O_{60.43}C_{18}N_3H_{81.86}$
Formula weight	2283.89
Crystal size	0.20 x 0.08 x 0.08 mm ³
Color; Habit	light green; hexagonal plate
Crystal system; Space group	Hexagonal; $P6_3/m$
Unit cell dimensions	$a = 13.4541(9) \text{ \AA}$ $c = 27.755(2) \text{ \AA}$
Volume	4350.9(5) \AA^3
Z	2
Density (calculated)	1.743 Mg/m ³
Absorption coefficient	1.327 mm ⁻¹
F(000)	2304
Temperature	294(2) K
Wavelength	0.71073 \AA
Theta range for data collection	1.75 to 27.12°.
Index ranges	$-9 \leq h \leq 17$, $-17 \leq k \leq 14$, $-35 \leq l \leq 34$
Reflections collected	29726
Independent reflections	3290 [R(int) = 0.0376]
Completeness to theta = 27.12°	99.8 %
Absorption correction	multi-scan (SADABS)
Max. and min. transmission	0.746 and 0.589
Refinement method	Full-matrix least-squares on F ²
Data / restraints / parameters	3290 / 2 / 134
Goodness-of-fit on F ²	1.069
Weight scheme	$w = 1/[\sigma^2(F_o^2) + (0.0623P)^2 + 6.91P]$, where $P = [\max(F_o)^2 + 2(F_c)^2]/3$
Final R indices [I>2σ(I)]	R1 = 0.0422, wR2 = 0.1191
R indices (all data)	R1 = 0.0461, wR2 = 0.1222
Largest diff. peak and hole	1.539 and -0.478 e. \AA^{-3}

Single-Crystal Structure Analysis. Crystal of dimensions $0.20 \times 0.08 \times 0.08 \text{ mm}^3$ for **1** was selected for indexing and intensity data collection at 294 K. The diffraction measurement were performed on Bruker Smart Apex CCD diffractometer systems equipped with a normal focus, 3 kW sealed-tube X-ray source ($\lambda = 0.71073 \text{ \AA}$). Intensity data was collected in 1315 frames with increasing ω (0.3° per frame). Unit cell dimensions were determined by a least-square fit of 15716 reflections. Empirical absorption corrections based on symmetry-equivalent reflections were applied by using the SADABS program^a ($T_{min}/T_{max} = 0.589/0.746$). On the basis of systematic absences and statistics of intensity distribution, the space group was determined to be $P6_3/m$. The structure was solved by direct method with all non-hydrogen atoms located on electron-density maps. On the basis of results from bond-valance-sum calculations, the atoms O(10) and O(8) were assigned coordination water and hydroxyl oxygen atom, respectively. During the refinement, we found that the P(4) site was not fully occupied and the O(9) - P(4) - O(9) angle was about 114.5° , which was not a regular geometry of most O - P - O angle in phosphites. From the ICP-AES results we confirmed the existence of B and further located it coexisting 0.3 \AA near the P(4) site with an occupancy of 21.6%. H(1) to H(6) can be located on electron density map while H(7) was calculated on the basis of a riding model due to disorder on hydroxyl group. The final cycles of refinements including the atomic coordinates and anisotropic thermal parameters for all non-H atoms and fixed atomic coordinates and isotropic thermal parameters for H atoms converged at $R_1/wR_2 = 0.0422/0.1191$. Neutral-atom scattering factors were used for all the atoms. Anomalous dispersion and secondary extinction corrections were applied. All calculations were performed by using the PC version of the SHELXTL program package.^b Crystallographic data are listed in Table S1, and ORTEP drawings are shown in Figure 2.

^a G. M. Sheldrick, *SADABS*. Version 2.03. University of GoÈ ttingen, Germany, 2002.

^bG. M. Sheldrick, *Acta Crystallogr.*, 2008, **A64**, 112-122.

Table S2. Selected Bond Length (Å) for **1**

V(1)-O(1) (6x)	2.013(2)	P(1)-O(1)	1.530(2)
V(2)-O(5) ^a	1.964(2)	P(1)-O(2)	1.513(2)
V(2)-O(9)	1.983(2)	P(1)-O(3)	1.522(2)
V(2)-O(4)	1.989(2)	P(1)-H(1)	1.3718
V(2)-O(6) ^b	1.986(2)		
V(2)-O(3)	1.992(2)	P(2)-O(4)	1.515(2)
V(2)-O(10)	2.096(2)	P(2)-O(5)	1.506(2)
V(3)-O(2) (3x)	1.996(2)	P(2)-O(6)	1.522(2)
V(3)-O(7) (3x)	2.005(3)	P(2)-H(2)	1.4665
P(3)-O(7) (2x)	1.478(2)	P(4)-O(9) (3x)	1.527(2)
P(3)-O(8) ^c	1.53(1)	P(4)-H(4)	1.2767
P(3)-O(8) ^{'c}	1.53(2)		
P(3)-H(3)	1.4781	B ^c -O(9) (3x)	1.487(5)

^a - x, - y + 1, - z + 1. ^b y, - x + y, - z + 1.

^c occupancy for O(8) and O(8)' are 0.65 and 0.35 and for B 0.22, respectively.

Table S3. ICP-AES data

batch\ppm	V	B	P
1	777	2.8	885
2	2573	3.68	2976
3	325	9.84	384
4	328	10.7	387

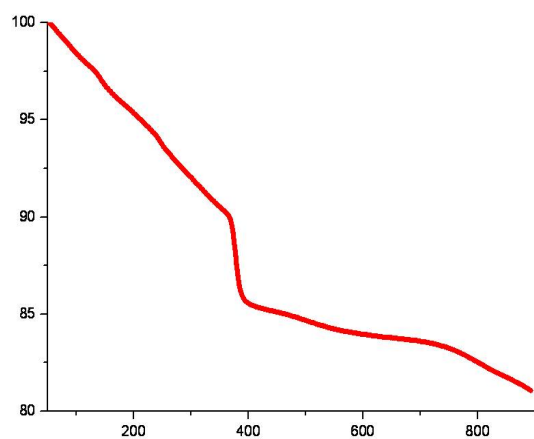


Figure S1. TG curves of compound **1**

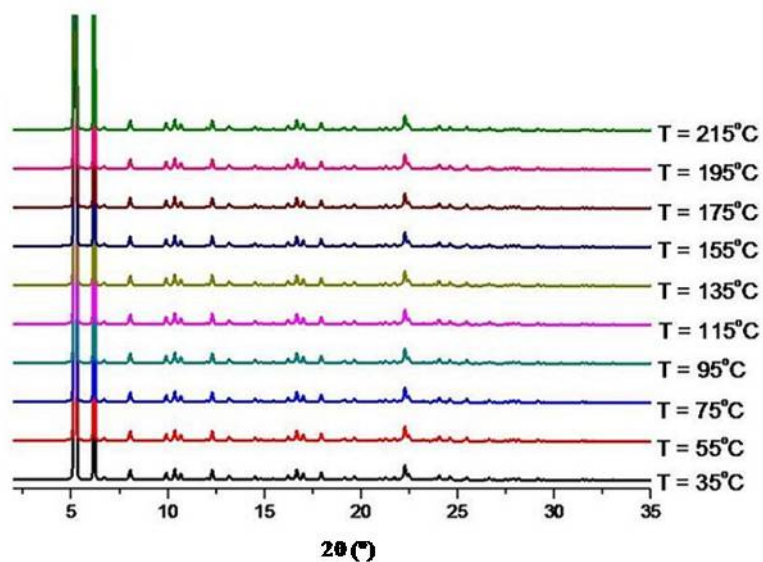
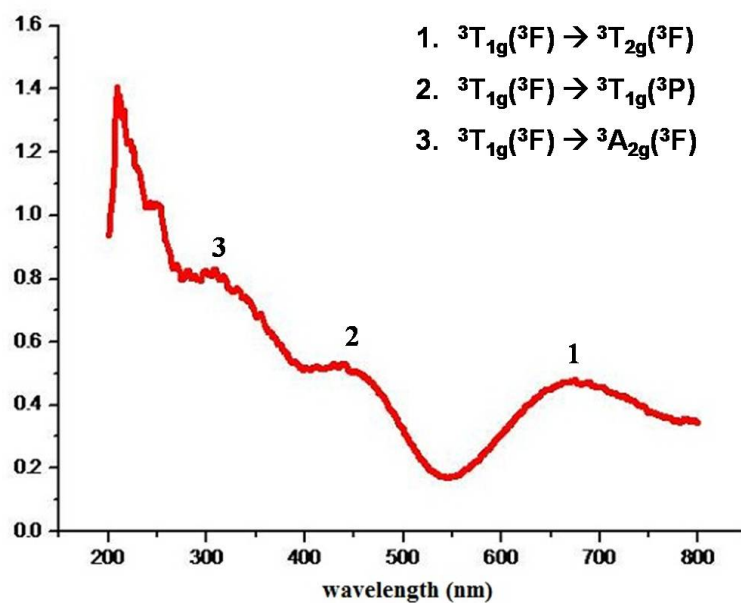


Figure S2. Variable-temperature powder X-ray diffraction patterns ($\lambda = 1.0332 \text{ \AA}$) of compound **1**.

(a)



(b)

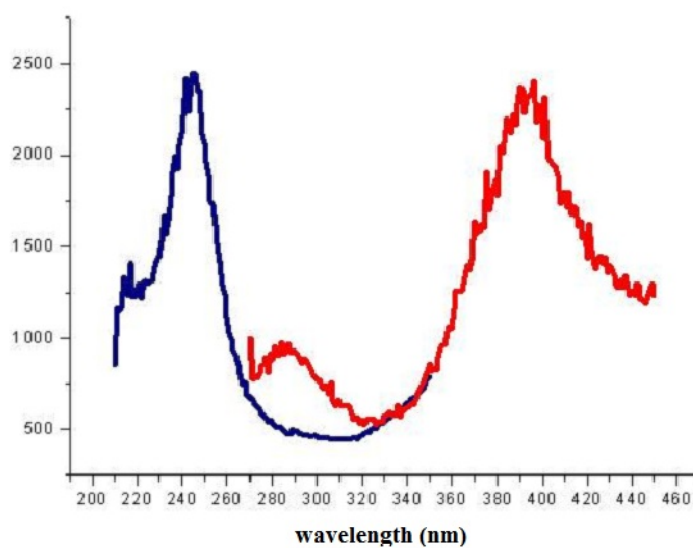
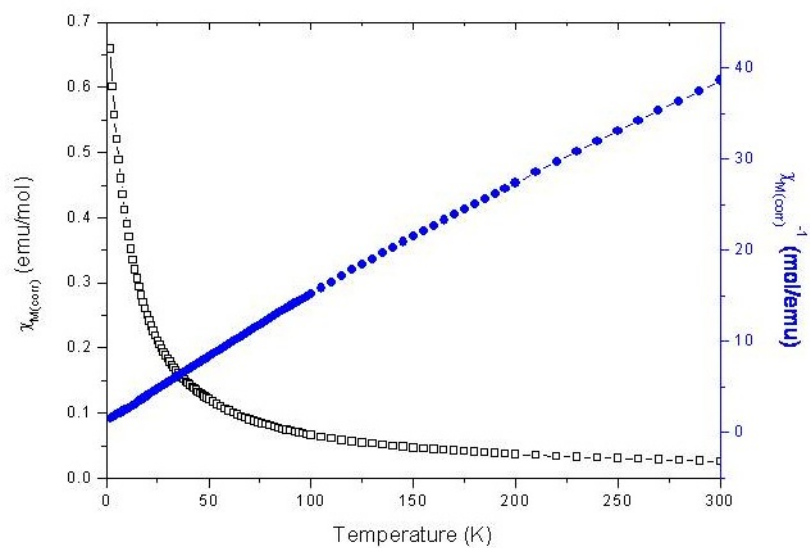


Figure S3. (a) Reflectance UV-vis spectra and (b) photoluminescence spectra of compound 1.

(a)



(b)

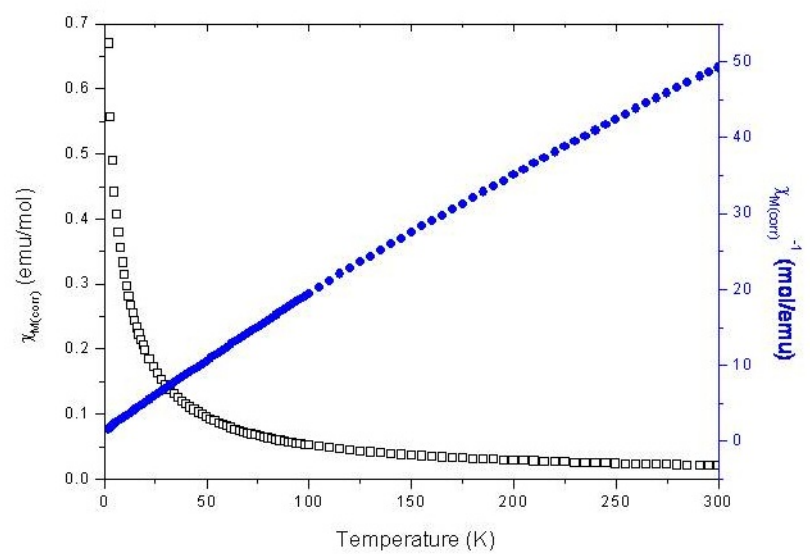
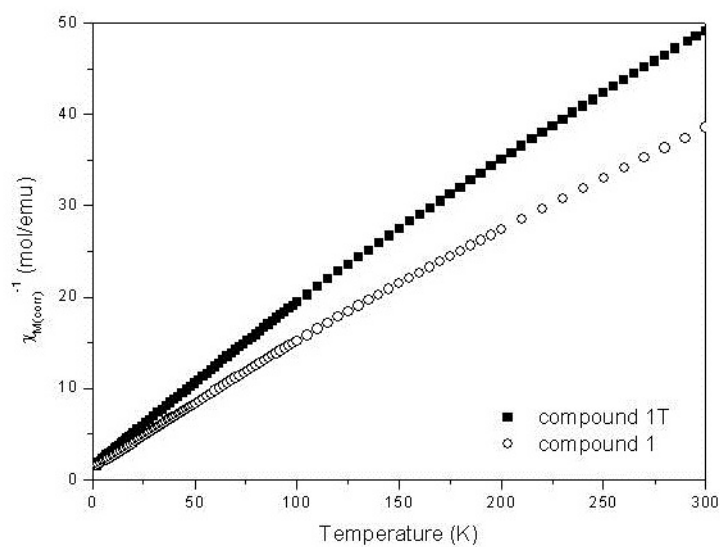


Figure S4. Susceptibility versus T curves for (a) **1**, and (b) **1T** (\square for χ_M versus T and \bullet for χ_M^{-1} versus T).

(a)



(b)

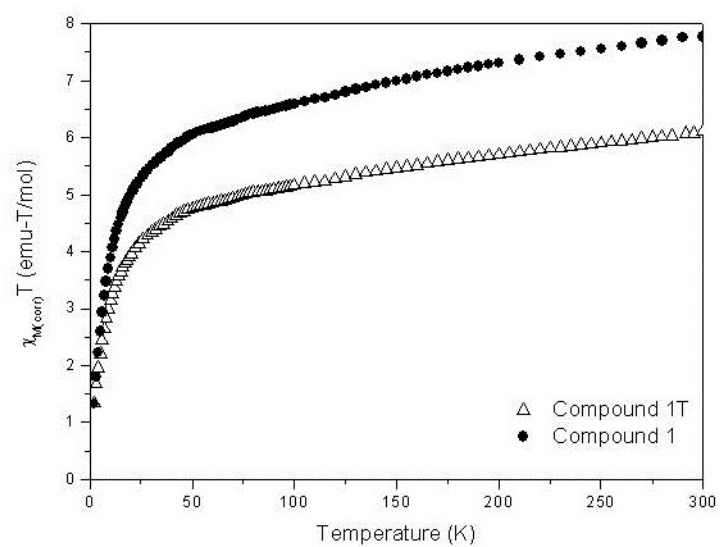


Figure S5. Plots of (a) χ_M^{-1} versus T , and (b) $\chi_M T$ versus T curves for **1** and **1T**.

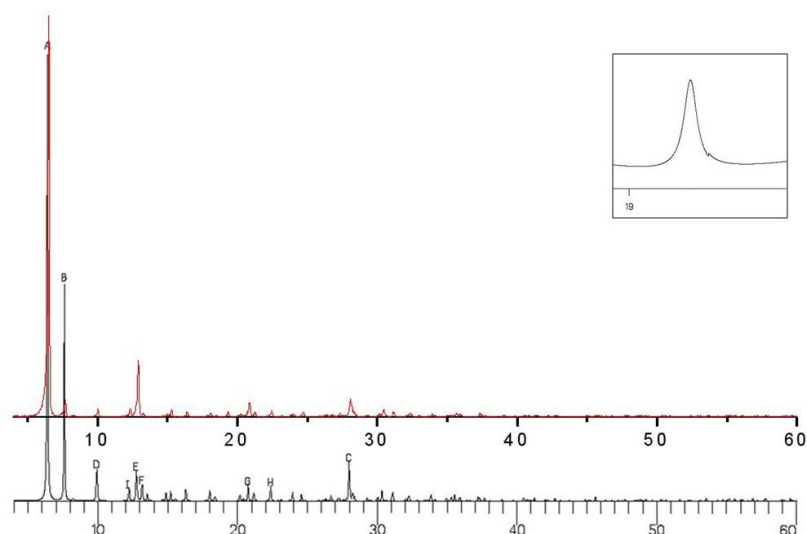


Figure S6. Simulated (bottom) and experimental (top) X-ray powder patterns for **1**, and the magnification part of the simulated pattern at 19.3° is shown in the inset.

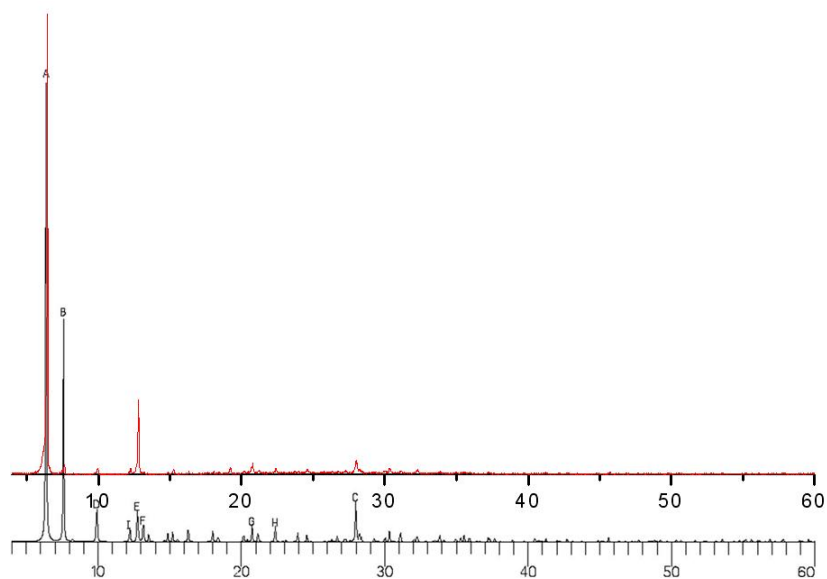


Figure S7. Comparable simulated (bottom) and experimental (top) powder patterns of **1** and the isostructure prepared with chpa, respectively.

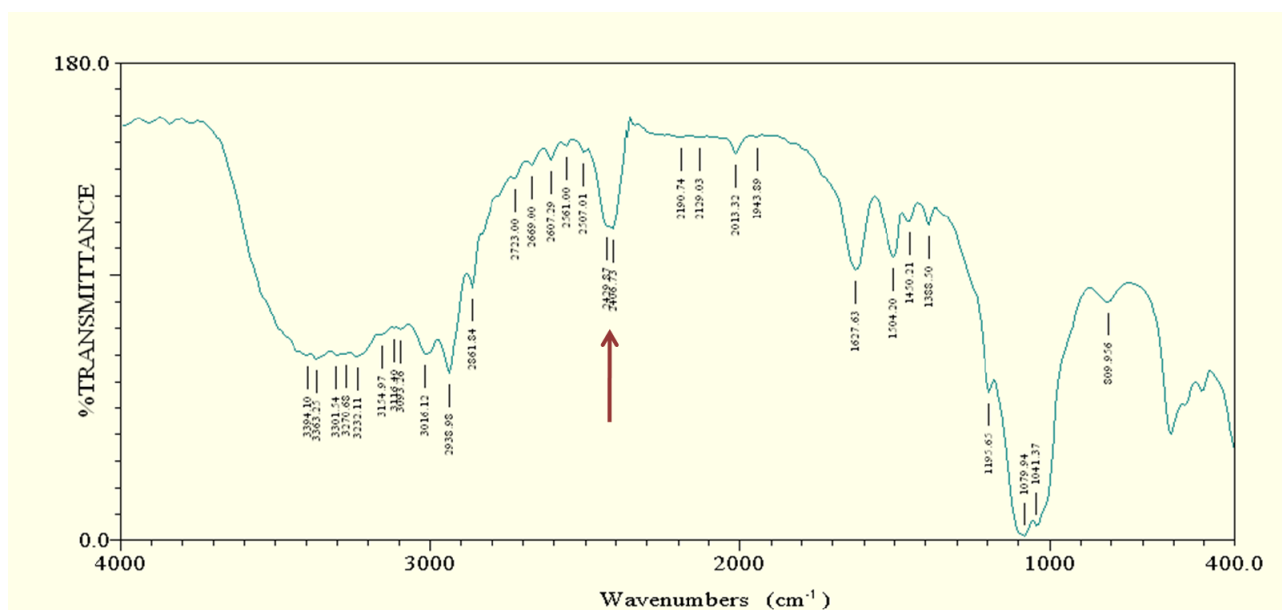


Figure S8. FTIR spectrum for **1**. The broad band indicated by red arrow is assigned to the typical P-H stretching vibration in phosphite groups.